

Investigating mass segregation process in globular clusters with Blue Straggler Stars: the impact of dark remnants

Emiliano Alessandrini¹, Barbara Lanzoni¹, Francesco R. Ferraro¹, Paolo Miocchi¹, Enrico Vesperini²

¹ *Dept. of Physics and Astronomy, University of Bologna, viale Berti Pichat, 6/2.* ² *Dept. of Astronomy, Indiana University, Bloomington, IN, 47401, USA.*

19 sept 2016

ABSTRACT

We present the results of a set of N-body simulations aimed at exploring how the process of mass segregation (as traced by the spatial distribution of blue straggler stars, BSSs) is affected by the presence of a population of heavy dark remnants (as neutron stars and black holes). To this end, clusters characterized by different initial concentrations and different fractions of dark remnants have been modeled. We find that an increasing fraction of stellar-mass black holes significantly delays the mass segregation of BSSs and the visible stellar component. In order to trace the evolution of BSS segregation, we introduce a new parameter (A^+) that can be easily measured when the cumulative radial distribution of these stars and a reference population are available. Our simulations show that A^+ might also be used as an approximate indicator of the time remaining to the core collapse of the visible component.

Subject headings: stellar dynamics — globular clusters: general — methods: n-body simulations

1. Introduction

Mass segregation is one of the manifestations of two-body relaxation in collisional stellar systems. Kinetic energy exchanges between stars with different masses cause a slowing down of the heaviest one, which spirals toward the centre of the system in favour of a velocity enhancement of the lighter one, which, instead, migrates toward the outskirt. Since the time scale of this process is the dynamical friction (DF) timescale t_{DF} (Chandrasekhar 1943), which depends on the local velocity dispersion and (especially) on the local density of the cluster (e.g., Binney & Tremaine 2008; Alessandrini et al. 2014), it is natural to expect different stellar systems to show different levels of mass segregation.

In this respect, Blue Straggler Stars (BSSs) have been used as powerful observational test particles to probe mass segregation in globular clusters (GCs; e.g., Mapelli et al. 2004, 2006; Ferraro et al. 1993, 1997, 2004, 2006b; Lanzoni et al. 2007a,b; Dalessandro et al. 2008; Beccari et al. 2011). This is because BSSs in GCs have a mass of $\sim 1.2 - 1.4M_{\odot}$ (Shara et al. 1997; Ferraro et al. 2006a; Lanzoni et al. 2007a; Fiorentino et al. 2014) which is larger than the main-sequence turn-off (MS-TO) mass and the average stellar mass in the system ($0.8M_{\odot}$ and $\sim 0.5M_{\odot}$, respectively). Hence, BSSs experience significant DF against "normal" cluster stars. Moreover, these objects are relatively bright, with visual magnitudes up to 2.5 dex above the MS-TO point (e.g., Sandage 1953; Ferraro et al. 1993; Lanzoni et al. 2007a; Dalessandro et al. 2012), and they can be efficiently distinguished from the normal low-mass stars in the cluster. Indeed, previous works largely demonstrated that BSSs tend to be more centrally concentrated than normal cluster populations (e.g., Ferraro et al. 1999), and different levels of segregation have been found in different GCs

(see, e.g., Figure 2 in Ferraro et al. 2003). Recently Ferraro et al. (2012) proposed to use the shape of the normalized BSS radial distribution¹ as an indicator of the level of dynamical evolution experienced by a stellar system.

Following this approach GCs can be grouped in three main families (*Family I, II and III*) of increasing dynamical ages on the basis of the different shapes of their BSS radial distribution. In the scenario proposed by Ferraro et al. (2012), DF is the main phenomenon that drives the BSS sedimentation toward the center of the system. Hence, *Family I GCs*, where BSSs follow the same radial distribution of the reference population, are dynamically young systems, where DF has not started yet to segregate these heavy objects, not even those orbiting the most central regions. In *Family II GCs*, where the BSS radial distribution is bimodal with a central peak, a minimum in the intermediate region, followed by a rising branch in the external part, the action of DF progressively affected BSSs at increasingly larger distances from the centre: these systems are dynamically intermediate-age GCs. In particular, four different *sub-Families II*, with progressively increasing dynamical ages according to the increasing radial position of the minimum of their BSS distribution, have been defined by Ferraro et al. (2012; see their Figure 2). Finally, in *Family III GCs*, where the BSS radial distribution shows only the central peak and then monotonically decreases at increasing distance from the cluster center, DF nominally segregated the entire population of BSSs: these are dynamically-old GCs.

Theoretical confirmations of this result have been searched by means of semi-analytic and numerical approaches. Alessandrini et al. (2014) excluded the possibility that the shape of the BSS radial distribution in Family II clusters is due to a combination of different DF times for different mass groups in a multi-mass system, thus confirming that the scenario proposed in Ferraro et al. (2012) is the most likely explanation of the observed shapes of the BSS distribution. The recent numerical work by Miocchi et al. (2015) provided some additional support to the observations, confirming the formation of a sharp central peak, which remains a stable feature over time, regardless of the initial concentration of the system. In spite of a noisy behaviour, a bimodal distribution is seen in several cases, and in the most advanced stages, the distribution becomes monotonic. However, in that work, the minimum of the BSS distribution is not always easily identifiable, and its outward migration occurs over a very short timescale, thus suggesting an insufficient level of realism of the adopted models. Admittedly, in Miocchi et al. (2015) the total number of particles was limited to only $N = 10^4$, and the mass spectrum was roughly modelled with only three mass bins. Moreover no populations of white dwarfs (WDs) and dark remnants (DRs), composed of neutron stars (NSs) and stellar mass black holes (BHs) were included. The dark component (BHs and NSs) is thought to substantially influence the cluster dynamics and structural properties (Sigurdsson & Hernquist 1993; Mackey et al. 2007, 2008; Morscher et al. 2015). In fact, since their masses are significantly larger than the average, DRs are thought to be the main drivers of the cluster core-collapse (CC) phase, forming close binaries that strongly interact dynamically with the other stars approaching the core during the evolution.

Hence, for the proper interpretation of the observational results, more realistic models of GCs are needed. In the present paper we discuss a set of simulations that, with respect to those in Miocchi et al. (2015), include (i) a significantly larger number ($N \simeq 10^5$) of particles, (ii) a much finer mass-spectrum obtained from the evolution of a Kroupa (2001) Initial Mass Function (IMF), and (iii) a population of DRs. The number of DRs in present-day GCs is poorly constrained and, during the last 30 years, many authors have addressed the problem of how many NSs (e.g. Hut et al. 1991; Drukier 1996; Davies & Hansen 1998; Pfahl et al. 2002; Podsiadlowski et al. 2005) and BHs (e.g., Sigurdsson & Hernquist 1993; O’Leary et al. 2006; Moody & Sigurdsson 2009; Repetto et al. 2012; Morscher et al. 2013; Sippel & Hurley 2013) are re-

¹With “normalized BSS distribution” here we indicate the double normalized ratio defined in Ferraro et al. (1993)

tained during the evolution of the cluster, in what is called the *retention problem*. For this reason, we performed simulations with different fractions of NSs and BHs. We emphasize that the models presented here are still idealized and aimed at exploring some fundamental aspects of the mass segregation process; additional ingredients (such as a population of primordial binaries or the effect of an external tidal field) are needed to approach more realistic models of GCs, and they will be the goal of forthcoming papers. By taking into account the limitations that are present also in the current approach, instead of following the evolution of the shape of the BSS distribution, here we focus on the definition of a new parameter able to quantify the level of sedimentation of BSSs toward the cluster center. The paper is organized as follows: in Section 2 we present our set of N-body models, describing the initial conditions of our simulations; in Sections 3.1–3.2 we discuss the time evolution of the Lagrangian radii and the cumulative radial distributions of BSSs and reference stars; in Sections 3.3 we define a new mass segregation indicator and discuss its time dependence. Section 4 summarizes the results obtained and future perspectives.

2. N-body models

The simulations exploit the Graphic Processing Unit (GPU) version of the direct N -body code **NBODY6** (Nitadori & Aarseth 2012) on the **BIGRED2** supercomputer at Indiana University, Bloomington. We performed ten different runs in order to explore both the effect of various percentages of DRs, and the effect of different cluster concentrations, on GC dynamical evolution.

The initial conditions have been built as follows. Starting from 99700 stars belonging to a Kroupa (2001) IMF, in the mass interval $m = [0.1, 100]M_{\odot}$ and assuming a metallicity $Z = 0.001$, we evolved the system for 12 Gyr, by means of the stellar evolution recipes implemented in the SSE version of the software **McLuster** (Hurley et al. 2000, 2002; Küpper et al. 2011). This procedure generated a population of WDs and DRs descending from the evolution of stars with initial masses $m > 0.8M_{\odot}$. In particular, NSs have masses peaked at $1.4M_{\odot}$, with a tail up to $2.5M_{\odot}$, while BH masses range between $2.5M_{\odot}$ and $\sim 25M_{\odot}$. To all the runs we also added 300 BSSs, modeled as single particles with a mass of $1.2M_{\odot}$. The number of BSSs in our runs, although being overabundant with respect to what observed in real GCs, guarantees enough statistics to limit stochastic noise in the results. We assume the particles follow a King (1966) model distribution with no primordial mass segregation. In order to explore the effect of different concentrations, we have chosen two different values of the King central dimensionless potential: $W_0 = 5$ and $W_0 = 8$.

With the aim of exploring how cluster dynamics depends on the presence and content of heavy objects, and to isolate the effect of BHs from that of NSs, for each of the adopted W_0 values we ran five simulations by varying, in the initial conditions, the percentage of DRs retained within the system: (i) in simulations $S_0^{W_0}$ (with $W_0 = 5, 8$) no DRs have been retained (hence, BSSs are the most massive objects in the cluster); (ii) in runs $S_{10}^{W_0}$ and $S_{30}^{W_0}$ we assumed that 10% and 30%, respectively, of NSs have been retained, while all BHs have been ejected; (iii) in simulations $S_{10\bullet}^{W_0}$ and $S_{30\bullet}^{W_0}$ we assumed that 10% and 30%, respectively, of NSs and BHs have been retained. The number of NSs, BHs, and BSSs in the initial conditions of each run are summarized in Table 1.

3. Results

3.1. Evolution of the Lagrangian Radii

We start the presentation of our results with a brief description of the evolution of the structural properties of our simulated clusters, and the effects of the presence of DRs. Figures 1 and 2 show the evolution of the 5%, 10% and 50% number Lagrangian radii of particles belonging to different populations in the simulations with no DRs and in those also including BHs, for $W_0 = 5$ and $W_0 = 8$, respectively. In particular, we compare the evolution of the Lagrangian radii of BSSs (i.e., all the particles with mass $m = 1.2 M_\odot$; blue lines), of what we call *reference* population (REF), corresponding to all the particles with masses between 0.75 and $0.84 M_\odot$ (red lines), and of the overall system, including all particles irrespective of their masses (grey lines). Moreover, for the runs with BHs, we also show in black the evolution of the DR population ($m > 1.4 M_\odot$). The figures clearly show that the cluster dynamical evolution is highly affected by the presence and amount of DRs, and also depends on the initial concentration of the system. Quite interestingly, this is true not only in the innermost cluster regions (as sampled by the 5% and 10% Lagrangian radii), but the effects also extend much outward, with large differences even at radial distances including 50% of the populations.

The analysis of the results obtained for $W_0 = 5$ (Fig. 1) shows that if no DRs are present (left-hand column) BSSs drive the cluster toward CC. This is indeed expected (see also Miocchi et al. 2015), since in that case, BSSs are the most massive objects within the system. The time evolution of the Lagrangian radii in the cases where only NSs are retained (namely, simulations S_{10}^5 and S_{30}^5) is very similar to that with no DRs (thus, we provide no explicit figures for these runs), since the large majority of NSs has masses comparable to that of BSSs. Hence, the main effect of including a DR population made of NSs only is that the collapse is driven by these objects and BSSs segregate just at a slightly slower rate than in the case with no DRs at all. In the $S_{10\bullet}^5$ and even more in the $S_{30\bullet}^5$ simulations, instead, DRs undergo a rapid decoupling from the other populations, forming a subsystem that quickly sinks toward the centre (see the black curves in the central and the right columns of Fig. 1). Clearly this behaviour is due to the subsystem of BHs, which have masses significantly larger than BSSs and NSs. Analogous results have been found and discussed also by Sigurdsson & Hernquist (1993) and Kulkarni et al. (1993), and again very recently by Banerjee et al. (2010) and Breen & Heggie (2013b). Interestingly, the effect of BHs on the time evolution of the BSS and REF Lagrangian radii is negligible if a retention fraction of only 10% is assumed. In fact, their value in the $S_{10\bullet}^5$ run is almost the same, at any fixed value of time $t/t_{\text{rh}0}$, as in the S_0^5 (and the S_{10}^5) case. In the $S_{10\bullet}^5$ simulation, after the initial phase of rapid DR decoupling, the inner Lagrangian radii of these heavy objects stay approximately constant up to $\sim 2.5 t_{\text{rh}0}$, then decrease steadily in time, closely followed by the Lagrangian radii of BSSs, which therefore start to participate in driving the overall cluster evolution, similarly to what happens in the S_0^5 run. Instead, for $f_{\text{DR}} = 30\%$ the effect played by BHs is much stronger. After the initial decoupling from the rest of the system, DRs evolve at almost constant Lagrangian radii for approximately 6 initial relaxation times, while the other stellar components migrate much more gently inward: the Lagrangian radii of all populations are systematically larger, at the same evolutionary time, with respect to what observed in the $S_{10\bullet}^5$ case, and the difference between the Lagrangian radii of the BSS and the REF populations is smaller. The Lagrangian radii of BSSs start to approach those of DRs at $\sim 6 t_{\text{rh}0}$, while the same happens much earlier in the $S_{10\bullet}^5$ run. The overall system reacts with a continuous expansion of r_{50} (grey line in the bottom right panel). The presence and the amount of BHs in the system has a strong impact on the rate at which the dynamical evolution of BSSs and REFs proceeds: in particular, the evolution of the level of mass segregation of the BSS population is increasingly inhibited and delayed as the adopted DR retention fraction increases. In fact, while the time of CC of the visible component is

$\sim 4.4 t_{\text{rh}0}$ if no DRs or only NSs are present, in the simulations including also BHs, it increases to ~ 5.2 for a 10% DR retention fraction, and further to ~ 7.5 for $f_{\text{DR}} = 30\%$. These behaviours can be explained as an effect of dynamical heating due to the population of BHs, which inhibits mass segregation. It is interesting to note that the inhibition of the mass segregation, due to the heating from a BH subsystem, resembles what Baumgardt et al. (2004), Trenti et al. (2007) and Gill et al. (2008) have found in the presence of an intermediate-mass black hole (IMBH). A recent study by Peuten et al. (2016) has also shown that the lack of segregation observed in NGC 6101 might be due to a population of BHs, a result consistent with our findings.

Similar general comments as above also apply to the case of a much more concentrated system ($W_0 = 8$, in place of $W_0 = 5$), where the impact of DRs including a population of BHs is even more apparent (see Fig. 2). Overall the time evolution is much faster than in the $W_0 = 5$ case, indicating that increasing the cluster concentration accelerates the dynamical evolution of the system. If DRs are absent, the inner Lagrangian radii (r_5 and r_{10}) of both BSSs and REF stars rapidly decrease in time until the CC (the rapid fluctuation in r_5 and r_{10} are simply a consequence of the ejection of BSS binaries), while r_{50} of the REF population remains almost constant during the entire evolution. If NSs and BHs are included (central and right-hand columns) all populations segregate much more slowly and the difference between the BSS and the REF Lagrangian radii is smaller at any fixed evolutionary times. In the $S_{30\bullet}^8$ run, DRs rapidly decouple from the rest of the system, then their inner Lagrangian radii expand significantly and start to re-contract only after $\sim 4 t_{\text{rh}0}$, closely followed by BSSs.

Hence, according to what expected, massive objects (especially stellar-mass BHs) are found to play a fundamental role in the cluster dynamics, driving the CC of visible stars and determining its timescale.

3.2. Cumulative radial distributions

The time evolution of the Lagrangian radii discussed in the previous section provides precious information about the processes of segregation and expansion of various stellar populations. Although our simulations are still idealized and not meant to be directly compared to observational data, it is important to identify and follow the evolution of mass segregation indicators that can be more easily adopted in observational studies of the segregation of BSS and REF populations. Many previous studies have shown that different GCs are characterized by different cumulative radial distributions, corresponding to different levels of BSS segregation in the central regions (e.g., Ferraro et al. 2004). Here we therefore study how the cumulative radial distributions of BSSs and REFs depend on the simulated cluster properties. In order to highlight the inner distance scale, where the effect of DF is the most evident, we choose to express the radial distance from the cluster centre in logarithmic units. Since in all simulations we assume no initial mass segregation (see Sect. 2), at $t = 0$ all populations are perfectly mixed and the BSS and the REF distributions are superimposed. However, as time increases, BSSs migrate toward the cluster centre more rapidly than the REF population (see Figs. 1 and 2) and the two corresponding cumulative radial distributions start to separate from each other.

For illustrative purposes, Figure 3 shows the cumulative radial distributions of BSSs and REFs (blue and red lines, respectively) for the $S_{30\bullet}^8$ run, at four different evolutionary times (normalized to the initial half-mass relaxation time of the run; see labels in the figure). For the sake of comparison, the radial distance is expressed in units of the half-mass radius of the REF population at the considered time. A notable feature in the figure is that the separation between the blue and the red lines increases with time, with the

BSS population always being more centrally segregated (i.e., with a steeper cumulative distribution) than the REF stars. This is due to DF that preferentially affects the heavier component (BSSs, with respect to REFs), making these objects more rapidly migrate toward the cluster centre.

Figure 4 compares the cumulative radial distributions obtained for the four models including BHs ($S_{10\bullet}^5$, $S_{30\bullet}^5$, $S_{10\bullet}^8$ and $S_{30\bullet}^8$) at a fixed evolutionary time, $t = 2.9 t_{\text{rh}0}$ (when the $S_{10\bullet}^8$ simulation stops). In line with what discussed in the previous sections, we find that BSSs are more centrally segregated for the lowest DR retention fraction (at fixed value of W_0) and for the largest cluster concentration (at fixed DR retention fraction). In particular, the accelerating effect on mass segregation due to a larger cluster concentration is clearly dominant in the case of a small population of DRs (10% retention fraction), while it is almost cancelled or even overcome if DRs become sufficiently numerous. In fact, for a fixed 30% retention fraction the cumulative radial distributions in the $W_0 = 5$ and $W_0 = 8$ cases are quite alike, with the latter becoming different from zero at only slightly lower radii than in the $W_0 = 5$ case (compare panels labeled with $S_{30\bullet}^5$ and $S_{30\bullet}^8$ in Fig. 4). Such an effect is even more apparent from the comparison of the $S_{10\bullet}^5$ and $S_{30\bullet}^8$ radial distributions: in spite of a smaller concentration (and thanks to a lower fraction of DRs) both stellar populations are more concentrated and the two cumulative distributions are more separated in the former case ($S_{10\bullet}^5$).

3.3. A new indicator of BSS segregation: A^+

The results discussed above suggest that the separation between the cumulative radial distributions can be used to measure the level of BSS central segregation with respect to a lighter cluster population taken as reference. We quantitatively define this new indicator as the area between the BSS and the REF cumulative radial distributions in the $\phi(r) - \log(r/r_{\text{hREF}})$ plane, and we name it A^+ .

For perfectly mixed populations (as it is the case at $t = 0$ in our models), such a parameter must be equal to zero. Then, A^+ is expected to become positive because the effect of DF is stronger on BSSs (heavier) than on the (lighter) REF stars, and the cumulative radial distributions of the two populations therefore start to separate from each other. According to the scenario presented by Ferraro et al. (2012), as time passes, the value of A^+ is expected to increase progressively, since BSSs orbiting at increasingly larger distances from the cluster centre sink to the bottom of the potential well and the increase of A^+ with time corresponds to the formation and the growth of the central peak of the normalized BSS distribution.

Fig. 5 shows that A^+ always increases with time and confirms that this parameter is indeed a sensitive indicator of the BSS sedimentation process. The figure confirms that NSs alone have a negligible impact on the rate of central BSS segregation: in fact, for a given value of W_0 , there is no significant difference between the models with different percentages of such objects (see, for instance, the red and the cyan dashed lines: S_{10}^5 and S_{30}^5 runs, respectively), nor between these models and those with the same W_0 but no DRs (compare the lines above with the grey one, S_0^5 , in the figure). Instead, BHs clearly appear to play a crucial role, significantly slowing down the evolution of the system (see colored solid lines in the figure). In particular, we note that for a given concentration (W_0) and time ($t/t_{\text{rh}0}$), the values of A^+ are larger for models with a smaller BH retention. On the other hand, for a given time and a given retention fraction, A^+ is larger for models with a larger initial concentration. At any given value of $t/t_{\text{rh}0}$, the largest values of A^+ are found for models with the largest concentration and the smallest BH retention fraction ($S_{10\bullet}^8$), while the smaller values of A^+ are found with lower concentration models with larger BH retention fraction ($S_{30\bullet}^5$). In addition, the parameter is larger in the $S_{10\bullet}^5$ case than in the $S_{30\bullet}^8$ run (at fixed time), demonstrating

that the (slowing) effect of a larger percentage of BHs is stronger than the (accelerating) effect of a larger cluster concentration. In our $W_0 = 8$ simulations all BHs are ejected from the system at the end of the run, while three and one BHs are still present at the end of the $S_{10\bullet}^5$ and $S_{30\bullet}^5$ simulations, respectively (see also Hoggie 2014; Hurley et al. 2016 for examples of models in which instead all or a large fraction of BHs are lost during the cluster evolution). The gradual loss of the initial population of BHs allows the BSS to segregate and A^+ to grow and reach values above 0.4-0.5 with a rate that is slower for increasing fractions of BHs. The simulations presented here serve the purpose of illustrating the general effect of a population of black holes on the process of segregation of BSS and the extent to which this effect depends on the fraction of BHs retained. The time evolution of A^+ might differ for clusters with different fractions of BHs. In particular, should the initial fraction of BHs be larger and/or the cluster structural properties allow to retain a larger fraction BHs than those adopted here (see e.g., Morscher et al. 2015; Chatterjee et al. 2016; Peuten et al. 2016), the rate of BSS segregation (and therefore the growth of A^+) could be slowed down and delayed more than what shown in the few illustrative cases we have explored.

All these properties are consistent with the conclusions of our discussion about the segregation process in terms of evolution of the Lagrangian radii (see Sect. 3.1) and show that the new parameter A^+ is a reliable indicator of the cluster dynamical evolution as traced by the BSS population.

Fig. 5 also shows that the time dependence of A^+ is characterized by two main regimes: an initial, slower phase, followed by a steeper trend toward the end of the simulations, at times approaching the CC time. This effect is more evident if BHs are included: the evolutionary times when the curves change regime are $t \approx 4.2, 5.5, 2$ and $6.2 t_{\text{rh}0}$ in the $S_{10\bullet}^5, S_{30\bullet}^5, S_{10\bullet}^8$ and $S_{30\bullet}^8$ runs, respectively. These epochs also correspond to the moment when the time dependence of the inner BSS Lagrangian radii also change slope, while those of the REF population evolve in a slower, smoother way (see Figs. 1 and 2). The fact that A^+ shows a regime of faster time dependence when the cluster is approaching the CC phase further demonstrates that it is an indicator of the level of BSS segregation and dynamical evolution of the system.

Figure 6 shows the evolution of A^+ as a function of time normalized to the CC time of the BSS and REF populations (t_{CC}). Interestingly, all the models fall on a relatively narrow band in this plane, irrespective of the amount and the mass of DRs they contain. This suggests that A^+ might be used as an approximate indicator of how far a cluster is from CC of the visible component.

4. Summary and conclusions

We performed a set of direct N-body simulations of GCs with $N \sim 10^5$ particles, with different initial concentrations ($W_0 = 5$ and $W_0 = 8$), and admitting a population of BSSs and different fractions of NSs and BHs (including the case of systems with no heavy DRs at all). BSSs are modelled as single particles of $1.2M_\odot$. The simulations have been used to investigate how a population of heavy objects affects mass segregation and the dynamical evolution of a cluster, and what can be learned from BSSs about these processes.

We have shown that the segregation of BSSs and of the most massive main sequence stars is significantly slowed down by the presence of BHs. This is due to the dynamical heating effect of these heavy objects that rapidly decouple from the other components, form a centrally concentrated sub-system and inhibit mass segregation of the less massive components. The effect of BHs stronger than that of concentration: in fact, in spite of a larger value of W_0 , the mass segregation process of currently visible stars (with masses $\leq 0.8M_\odot$) in the $S_{30\bullet}^8$ run is much slower than that of the $S_{10\bullet}^5$ simulation.

Because of their larger masses, BSSs are expected to be more affected by the mass segregation process and to be more centrally segregated than the REF population. This has been indeed observed in several previous studies, also showing that the level of BSS segregation (and thus the relative separation between the BSS and the REF cumulative radial distributions) varies from cluster to cluster (see, e.g., Figure 2 in Ferraro et al. 2003). In the framework of the dynamical clock (Ferraro et al. 2012), this is the result of DF, which favors the sedimentation of BSSs toward the cluster center, causing the formation of a central peak in the normalized BSS radial distribution. Here we have proposed the parameter A^+ as a new tool to measure this sedimentation level. We found that A^+ shows a clear increasing trend with time that well reflects the evolution of the Lagrangian radii observed in the various runs, with analogous dependences on the cluster concentration and the DR retention fraction. As the system evolves and loses part of the initial population of BHs, the level of BSS segregation grows at an increasing rate and diverge from that of the REF stars. As a consequence, the time dependence of A^+ shows a change in the slope. This demonstrates that A^+ is indeed a very good tracer of BSS segregation, and can reveal both how advanced BSS segregation is and the extent to which the presence of a DR population has inhibited it. In all the considered simulations, the parameter assumes comparable values at any fixed fraction of the CC time (see Fig. 6). Hence, it seems to be a good indicator of the time remaining to the CC of the visible component, reasonably irrespective of the initial concentration and DR content of the system.

In order to illustrate how the strength of the mass segregation depends on the populations chosen, in Fig. 7 we compare the time evolution of the A^+ parameter calculated for BSSs and REF stars (black curves, the same as those plotted in colors in Fig. 5) and the time evolution of the A^+ parameter calculated using REF and $m = 0.4M_\odot$ particles (grey curves). In the former case the mass ratio between the two populations is 1.5, while it is larger (equal to 2) in the latter. While in both cases A^+ increases with time, the effect is much stronger in the former. This is because, in spite of a smaller mass ratio between the former populations (BSSs and REFs), the relative effect of mass segregation on these components is stronger than that on REF and $0.4M_\odot$ stars. This behaviour suggests that BSSs are more powerful observational tracers of dynamical evolution than, for instance, main sequence stars.

Although our simulations are still idealized, they illustrate the general expected evolution of the A^+ parameter, and its dependence on the evolutionary stage of a cluster and its DR content. A larger exploration of the parameter space, including a wider grid of values for W_0 and f_{DR} , a population of primordial binaries and the effect of a host galaxy tidal field, is needed before drawing more quantitative conclusions. These aspects will be studied in future investigations. On the observational side, we just provided the first empirical determination of A^+ in a sample 25 of Galactic GCs, demonstrating that it shows tight correlations both with the radial position of the minimum of their BSS distribution and with the cluster central relaxation time (Lanzoni et al. 2016, ApJ submitted), further confirming that it is a powerful indicator of GC dynamical evolution.

Acknowledgements

This research is part of the project Cosmic-Lab (web site: <http://www.cosmic-lab.eu>) funded by the European Research Council (under contract ERC-2010-AdG-267675). EA thanks the *Marco Polo Project* of the Bologna University and the Indiana University for the hospitality during his stay in Bloomington, where part of this work was carried out. This research was supported in part by Lilly Endowment, Inc., through its support for the Indiana University Pervasive Technology Institute, and in part by the Indiana METACyt Initiative. The Indiana METACyt Initiative at IU is also supported in part by Lilly Endowment,

Inc. We warmly thank Dr. Jongsuk Hong for stimulating discussions and his support in running the N-body simulations. We also thank the anonymous Referee for useful comments that improved the presentation of the paper.

REFERENCES

- Alessandrini, E., Lanzoni, B., Miocchi, P., Ciotti, L., Ferraro, F. R., 2014, *ApJ*, 795, 169.
- Banerjee, S., Baumgardt, H., Kroupa, P., 2010, *MNRAS*, 402, 371.
- Baumgardt, H., Makino, J., Ebisuzaki, T., 2004, *ApJ*, 613, 1143.
- Beccari, G., Sollima, A., Ferraro, F. R., Lanzoni, B., Bellazzini, M., De Marchi, G., Valls-Gabaud, D., Rood, R. T., 2011, *ApJ*, 737, 3.
- Breen, P. G., Heggie, D., 2013a, *MNRAS*, 432, 2779.
- Breen, P. G., Heggie, D., 2013b, *MNRAS*, 436, 584.
- Binney, J., Tremaine, S., 2008, *Galactic Dynamics*. Princeton University Press, Princeton, USA.
- Chandrasekhar, S., 1943, *ApJ*, 97, 255.
- Chatterjee, S., Rodriguez, C., L., & Rasio, F., A. 2016, preprint (arXiv:1603.00884)
- Dalessandro, E., Lanzoni, B., Ferraro, F. R., Vespe, F., Bellazzini, M., Rood, R. T., 2008, *ApJ*, 681, 311.
- Dalessandro, E., Schiavon, R. P., Rood, R. T., Ferraro, F. R., Sohn, S. T., Lanzoni, B., O’Connell, R. W., 2012, *AJ*, 144, 126.
- Davies, M. B., Hansen, B. M. S., 1998, *MNRAS*, 301, 15.
- Drukier, G. A., 1996, *MNRAS*, 280, 498.
- Ferraro, F. R., Fusi Pecci, F., Cacciari, C., 1993, *AJ*, 106, 2324.
- Ferraro, F. R., Paltrinieri, B., Fusi Pecci, F., Cacciari, C., Dorman, B., Rood, R. T., Buonanno, R., Corsi, C. E., Burgarella, D., Laget, M., 1997, *A&A*, 324, 915.
- Ferraro, F. R., Paltrinieri, B., Rood, R. T., Dorman, B., 1999, *ApJ*, 522, 983.
- Ferraro, F. R., Sills, A., Rood, R. T., Paltrinieri, B., Buonanno, R., 2003, *ApJ*, 588, 464.
- Ferraro F. R., Beccari G., Rood, R. T., Bellazzini M., Sills A., Sabbi E., 2004 *ApJ*, 603, 127.
- Ferraro, F. R., Sabbi, E., Gratton R., Piotto, G., Lanzoni, B., Carretta, E., Rood, R. T., Sills, A., Fusi Pecci, F., Moehler, S., Beccari, G., Lucatello, S., Compagni, N., 2006a, *ApJ*, 647, L53.
- Ferraro, F. R., Sollima, A., Rood, R. T., Origlia, L., Pancino, E., Bellazzini, M., 2006b, *ApJ*, 638, 433.
- Ferraro, F. R., Lanzoni, B., Dalessandro, E., Beccari, G., Pasquato, M., Miocchi, P., Rood, R. T., Sigurdsson, S., Sills, A., Vesperini, E., Mapelli, M., Contreras, R., Sanna, N., Mucciarelli, A., 2012, *Nature*, 492, 393.
- Fiorentino, G., Lanzoni, B., Dalessandro, E., Ferraro, F. R., Bono, G., Marconi, M., 2014, *ApJ*, 783, 29.
- Gill, M., Trenti, M., Miller, M. C., van der Marel, R., Hamilton, D., Stiavelli, M., 2008, *ApJ*, 686, 303.
- Heggie, D., 2014, *MNRAS*, 445, 3435.

- Hurley, J. R., Pols, O. R., Tout, C. A., 2000, MNRAS, 315, 543.
- Hurley, J. R., Pols, O. R., Tout, C. A., 2002, MNRAS, 329, 897.
- Hurley, J. R., Sippel, A. C., Aarseth, S., Tout, C. A., 2016, *pasa*, 33, 36.
- Hurley et al. 2016 PASA, 33,36 (<http://arxiv.org/abs/1607.00641>)
- Hut, P., Murphy, B. W., Verbunt, F., 1991, A&A, 241, 137.
- King, I. R., 1966, AJ, 71, 64.
- Kroupa, P., 2001, MNRAS, 322, 231.
- Küpper, A. H. W., Maschberger, Th., Kroupa, P., Baumgardt, H., 2011, MNRAS, 417, 2300.
- Kulkarni, S. R., Hut, P., McMillan, S., 1993, Nature, 364, 421.
- Lanzoni, B., Sanna, N., Ferraro, F. R., Valenti, E., Beccari, G., Schiavon, R. P., Rood, R. T., Mapelli, M., Sigurdsson, S., 2007a, ApJ, 663, 1040.
- Lanzoni, B., Dalessandro, E., Ferraro, F. R., Mancini, C., Beccari, G., Rood, R. T., Mapelli, M., Sigurdsson, S., 2007b, ApJ, 663, 267.
- Mapelli, M., Sigurdsson, S., Colpi, M., Ferraro, F. R., Possenti, A., Rood, R. T.; Sills, A.; Beccari, G., 2004, ApJ, 605, L29.
- Mapelli, M., Sigurdsson, S., Ferraro, F. R., Colpi, M., Possenti, A., Lanzoni, B., 2006, MNRAS, 373, 361.
- Miocchi, P., Pasquato, M., Lanzoni, B., Ferraro, F. R., Dalessandro, E., Vesperini, E., Alessandrini, E., Lee, Y.-W., 2015, ApJ, 799, 44.
- Mackey, A. D., Wilkinson, M. I., Davies, M. B., Gilmore, G. F., 2007, MNRAS, 379, L40.
- Mackey, A. D., Wilkinson, M. I., Davies, M. B., Gilmore, G. F., 2008, MNRAS, 386, 65.
- Moody, K., & Sigurdsson, S., 2009, ApJ, 690, 1370.
- Morscher, M., Umbreit, S., Farr, W. M., Rasio, F. A., 2013, ApJ, 763, 15.
- Morscher, M., Bharath, P., Rodriguez, C., Rasio, F. A., Umbreit, S., 2015, ApJ, 800, 9.
- Nitadori, K., & Aarseth, S. J., 2012, MNRAS, 424, 545.
- O’Leary, R. M., Rasio, F. A., Fregeau, J. M., Ivanova, N., O’Shaughnessy, R., 2006, ApJ, 637, 937.
- Pfahl, E., Rappaport S., Podsiadlowski P., 2002, ApJ, 573, 283.
- Peuten, M., Zocchi, A., Gieles, M., Gualandris, A., Henault-Brunet, V., 2016, MNRAS, 462, 2333.
- Podsiadlowski P., Pfahl, E., Rappaport S., 2005, *ASP Conference Series*, 328.
- Repetto S., Davies, M. B., Sigurdsson S., 2012, MNRAS, 425, 2799.
- Sandage A. R., 1953, AJ, 58, 61.
- Shara, M. M., Saffer R. A., Livio M., 1997, ApJ, 489, 59.

Sigurdsson, S., Hernquist, L., 1993, *Nature*, 364, 423.

Sippel, A. C., Hurley, J. R., 2013, *MNRAS*, 430, L30.

Trenti, M., Ardi, E., Shin, M., Hut, P., 2007, *MNRAS*, 374, 857.

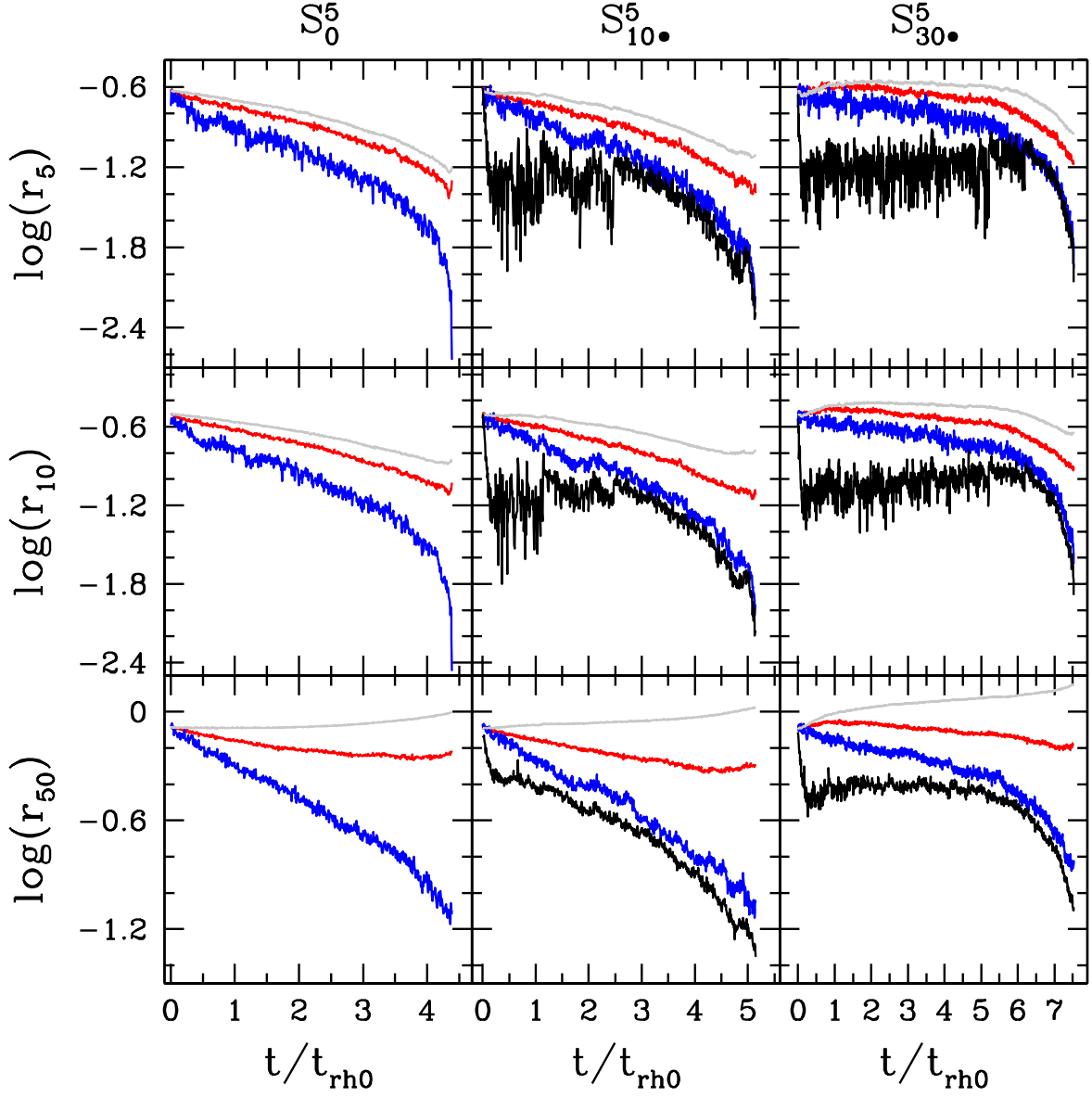


Fig. 1.— Evolution of the Lagrangian radii containing 5%, 10% and 50% (top, central and bottom panels, respectively) of the relative number of DRs (black), BSSs (blue), REF stars (red), and particles of any mass (grey), for the three runs with $W_0 = 5$ that include BHs. Time is normalized to the initial half-mass relaxation time $t_{\text{rh}0}$ of each run (see Table 1).

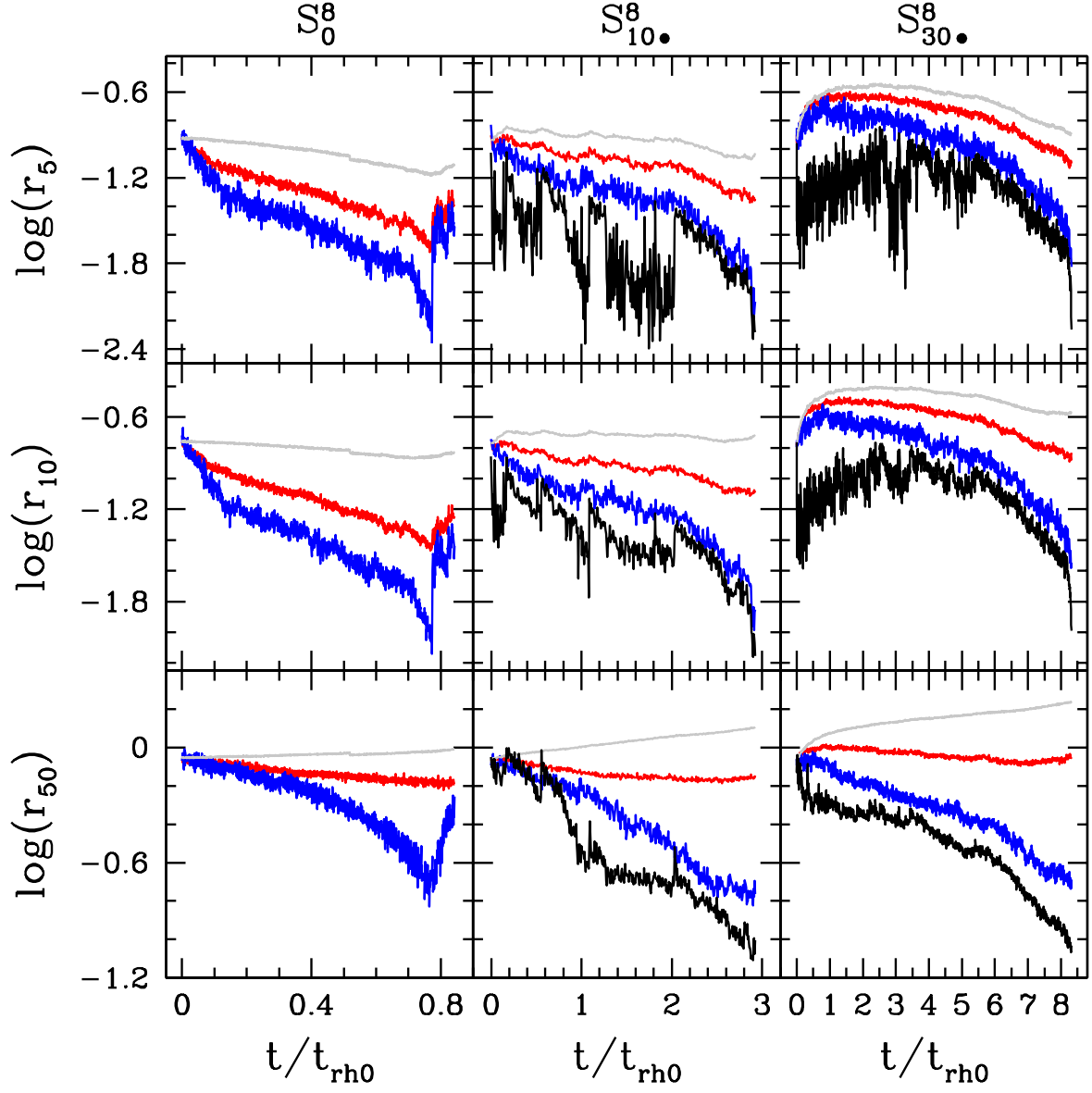


Fig. 2.— Same as Figure 1 for the runs with $W_0 = 8$ that include BHs.

Run	W_0	f_{DR} %	N_{NS0}	N_{BH0}	N_{BSS0}	N_{TOT}	t_{rh0}
S_0^5	5	0	0	0	300	10^5	1330.5
S_{10}^5	5	10	72	0	300	99161	1325.4
S_{30}^5	5	30	206	0	300	99295	1326.9
$S_{10\bullet}^5$	5	10	72	19	300	99180	1325.6
$S_{30\bullet}^5$	5	30	206	67	300	99362	1328.8
S_0^8	8	0	0	0	300	10^5	1471.7
S_{10}^8	8	10	71	0	300	99183	1465.3
S_{30}^8	8	30	200	0	300	99313	1466.9
$S_{10\bullet}^8$	8	10	71	17	300	99202	1470.6
$S_{30\bullet}^8$	8	30	200	65	300	99379	1467.8

Table 1: Initial conditions of the N-body simulations. For each run, the table lists the adopted name (column 1), the initial value of the King dimensionless potential W_0 (column 2), the initial retention fraction of DRs (column 3), the total number of DRs, BHs, BSSs and particles of any mass at $t = 0$ (columns 4–7), the initial half-mass relaxation time expressed in N-body units (column 8).

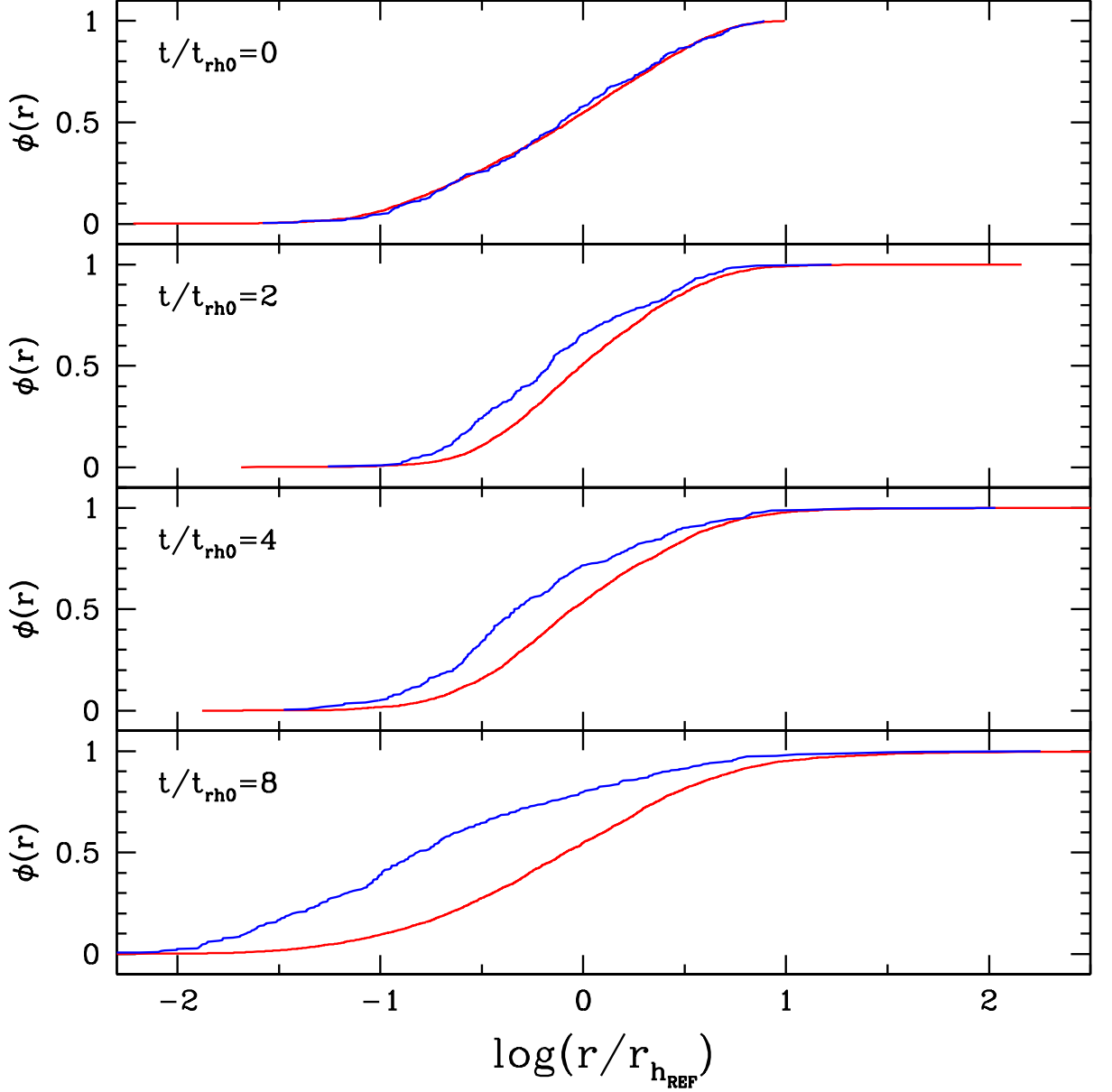


Fig. 3.— From top to bottom, time evolution of the cumulative radial distributions of BSSs (blue lines) and REF stars (red lines), for the $S_{30\bullet}^8$ simulation. The radial scale is logarithmic, with the radius normalized to the half-mass radius of the REF population measured at any considered evolutionary time (see labels). At $t = 0$ the two populations are perfectly mixed and their cumulative radial distributions superimposed. For increasing time, the two distributions become more and more separated due to the effect of mass segregation that preferentially segregates the heavier objects (BSSs) toward the clustre centre. The same qualitative trend is observed in all simulations.

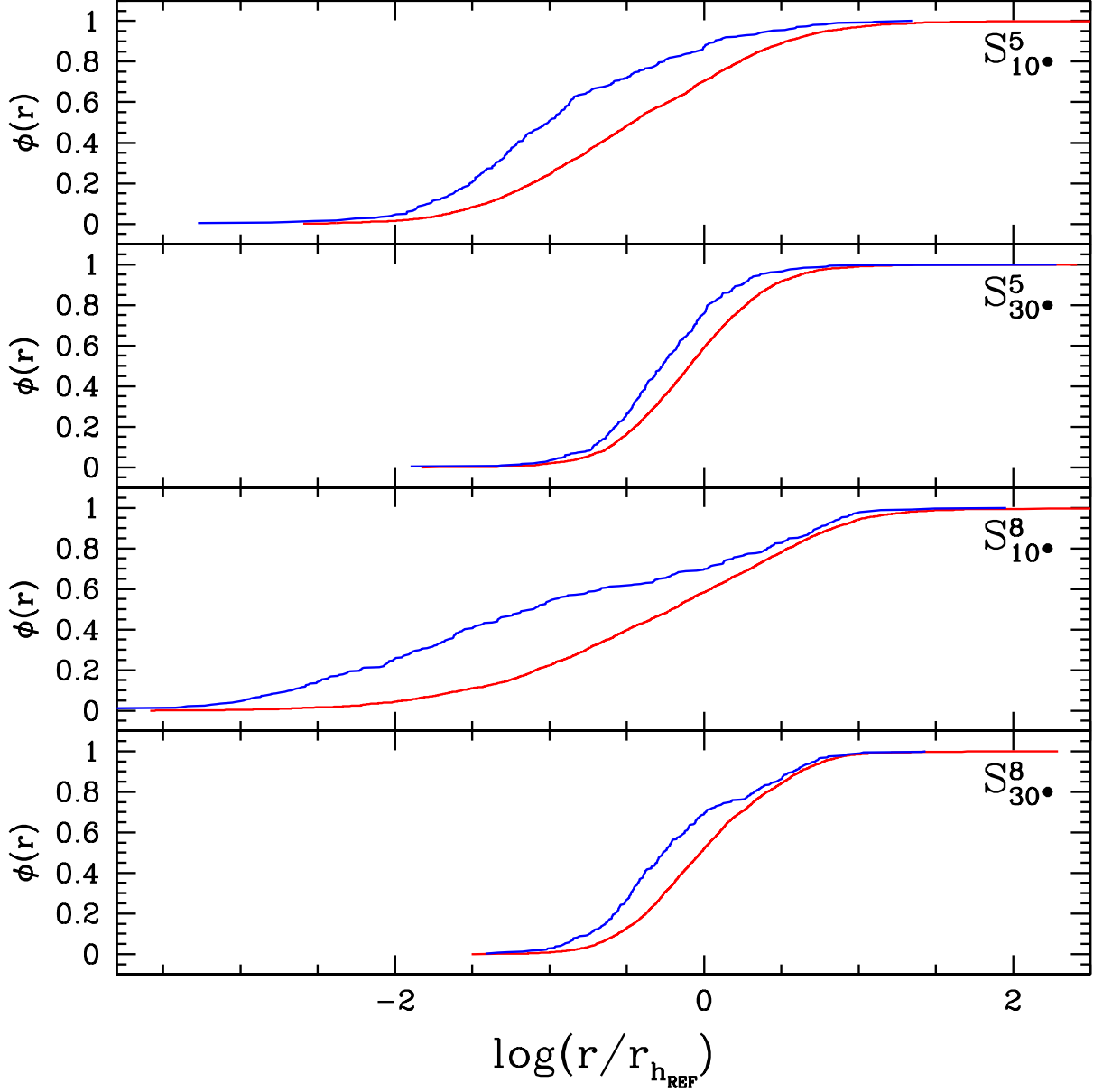


Fig. 4.— Comparison among the cumulative radial distribution of BSSs (blue lines) and REF stars (red lines) at the same evolutionary time ($t = 2.9 t_{\text{rh0}}$) in the four runs including BHs (see labels). The highest central concentration of BSSs (testified by both the lowest inner radius and the largest separation between the two distributions) is found for the $S^8_{10\bullet}$ run (which shows the fastest evolution: cfr with Figs. 1). The smallest central segregation of BSSs is observed in the $S^5_{30\bullet}$ cluster (which, in fact, shows the slowest dynamical evolution).

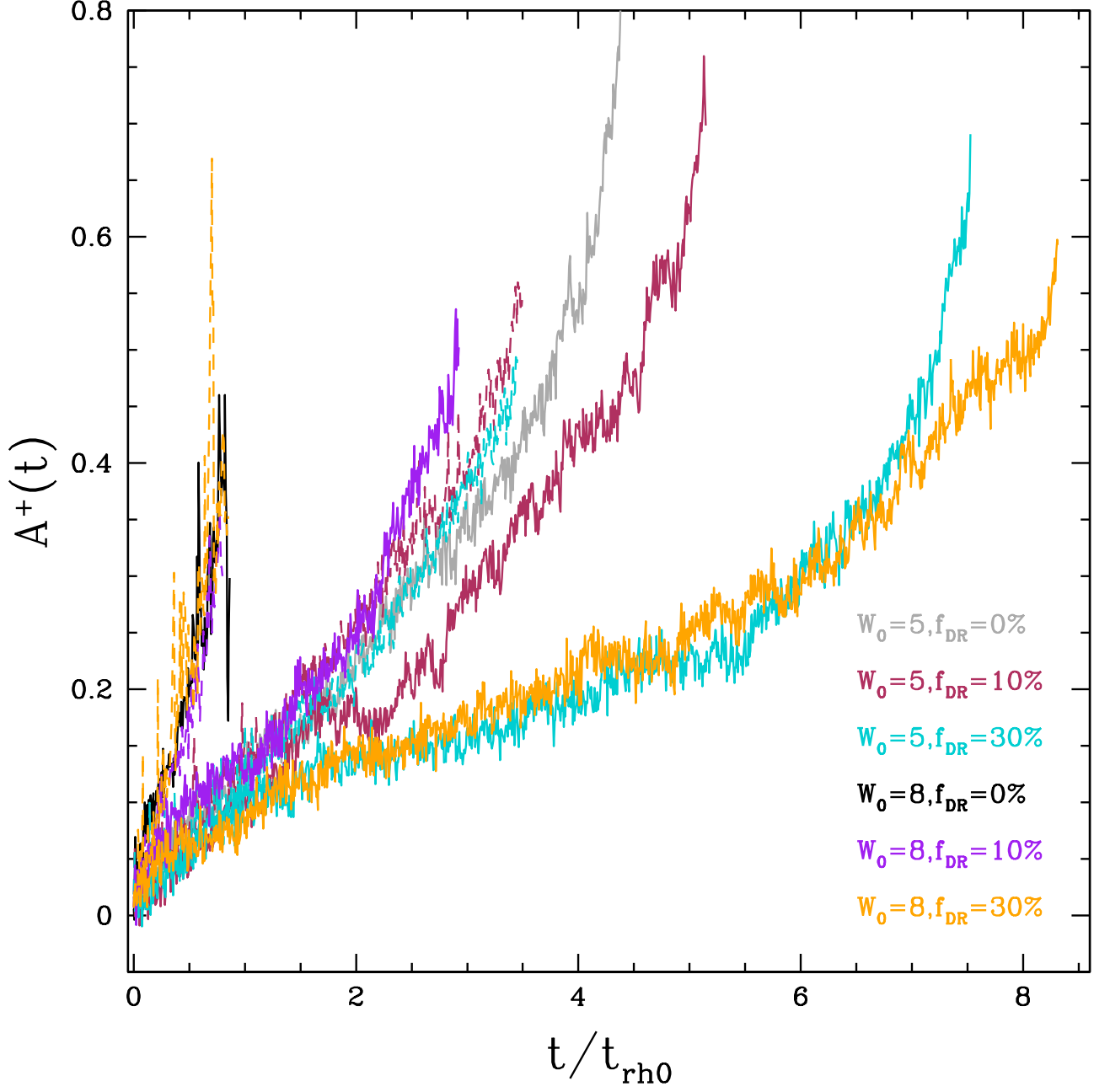


Fig. 5.— Evolution of A^+ as a function of the time normalized to $t_{\text{rh}0}$ in the all our models: simulations with no DRs are plotted in grey and black for the $W_0 = 5$ and $W_0 = 8$ cases, respectively; the dashed lines refer to models with only NSs, while the solid lines correspond to the simulations including both NSs and BHs (see the labels for the color code). A^+ increases with time as expected for a reliable mass segregation and dynamical evolution indicator (see Sect. 3.3).

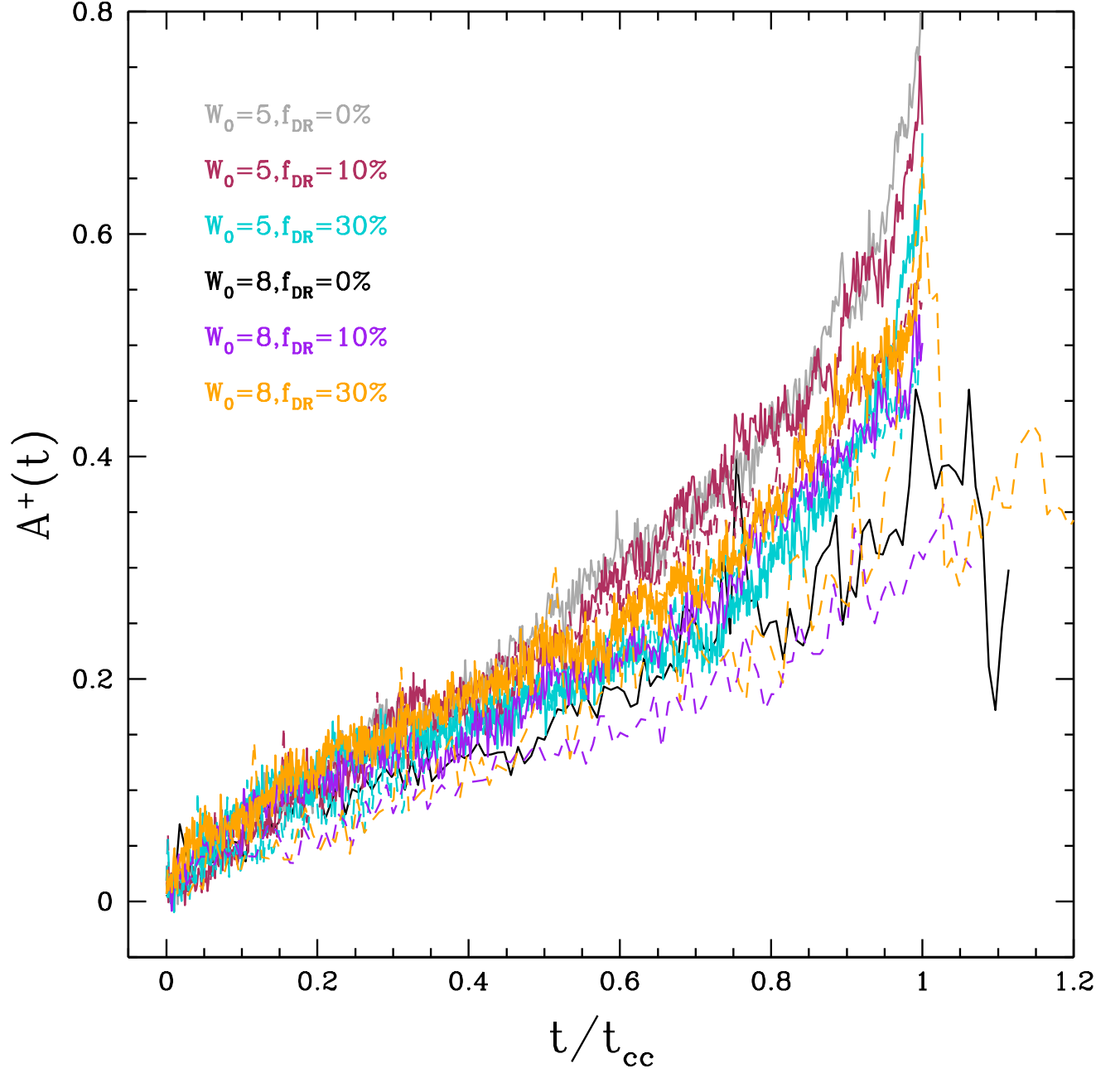


Fig. 6.— Same as Fig. 5, but with the time normalized to the CC time of BSSs and REF stars in every model (t_{CC}).

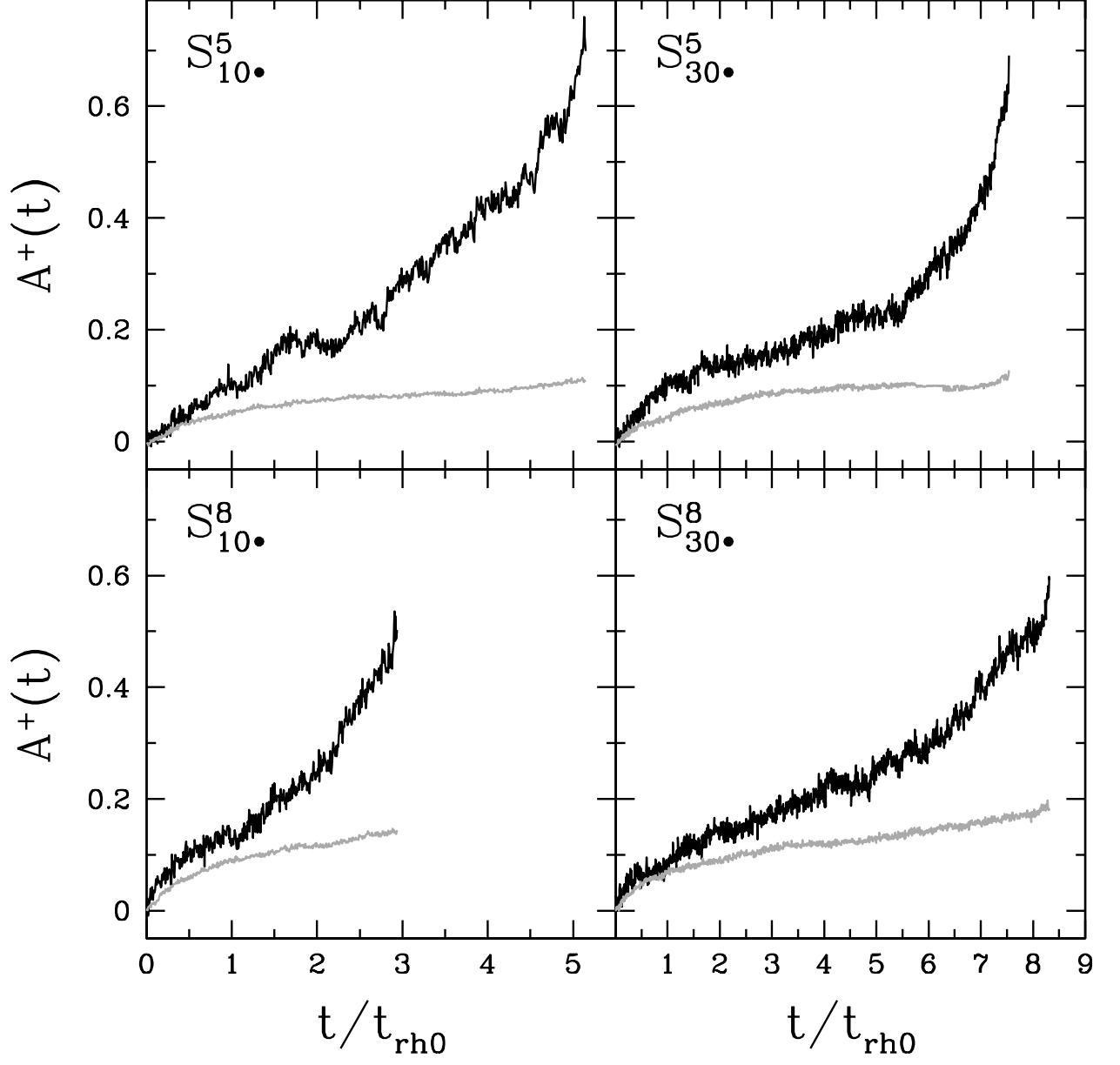


Fig. 7.— Time evolution of the parameter A^+ computed from two different pairs of populations for our set of simulations (see labels). The black curves are the same as the solid colored lines in Fig. 5 (obtained from the BSS and the REF populations in the models with BHs) while the grey lines mark the values of the area between the cumulative radial distributions of REF stars and $m = 0.4M_\odot$ particles.